SPE Flow Assurance Technology Congress
Rio de Janeiro, Brazil, November 15 – 18 2022

Experimental Characterization of the Dispersed bubbles in the Slug of an Air-water Slug Flow in a Vertical Pipe

Alexandre Gmyterco[1], Carolina C. Rodrigues[1], Paul A. D. Maldonando[1], Ernesto Mancilla[1], Roberto da Fonseca Junior[2], Marco J. da Silva[1], Rigoberto E. M. Morales[1*]
[1]Multiphase Flow Research Center (NUEM), Federal University of Technology – Paraná (UTFPR), Curitiba, Brazil
[2]CENPES/PDIEP/EE Petrobrás, Brazil, *rmorales@utfpr.edu.br

Abstract
Slug flow is one among the different flow patterns that two-phase flows can assume. This pattern is composed by a Taylor bubble and a liquid slug. Given the transient and intermittent behavior of this kind of flow, it becomes necessary to describe its characteristics. In this study, an experimental characterization of the slug flow in a 0.026-m ID, 14-m long vertical pipe was developed. Experiments for air and water were carried out, both the gas and liquid superficial velocities ranging from 0.2 to 1.5 m/s. The monitoring of the slug flow structures, was accomplished by using a wire-mesh resistive sensor. Close to this sensor, a high-speed camera was positioned in order to observe the shape of the Taylor bubbles. From the experimental data, a phenomenological analysis of the flow was developed as a function of the dimensionless Froude and Reynolds numbers. The mean diameter of the dispersed bubbles was computed as a function of the liquid flow inertia, and a decrease in their sizes with the increment of the Reynolds number was observed. Additionally, an increase in the Taylor bubble velocity as a function of the Reynolds number was observed.

Keywords
Slug-flow; dispersed-bubbles; Taylor-bubble-velocity

Introduction

Two-phase flows occur in Nature and in several industrial applications such as in the chemical, nuclear, geothermal, aerospace and oil industries. These flows present different spatial configurations, which depend on the liquid and gas flow rates, pipe geometry (i.e., diameter, shape) and physical properties of the fluids (densities, viscosities and surface tensions) [1]. Pipe inclination also affects the flow pattern because of the influence of the gravity on the phases. In vertical pipes, the flow patterns tend to be symmetrical around the pipe longitudinal axis, as gravity acts with the same intensity on the cross section. The flow patterns commonly found in the two-phase upward liquid-gas flow in vertical pipes can be classified as bubbly, slug, churn, annular, mist and dispersed bubble flows [2]. The transition between these flow patterns is governed by the increased gas flow rate, which induces the coalescence of the bubbles. Initially, cap bubbles of spherical shape are formed, which later coalesce, and form elongated bubbles, known as Taylor bubbles, which fill almost the entire cross-sectional area of the pipe.

The Taylor bubbles have a characteristic bullet shape, rising in a semi-periodic manner. These large bubbles are followed by liquid slugs, in whose bodies smaller dispersed bubbles can be found. In such case, a thin liquid film flowing downwards between the Taylor bubbles and the wall of the pipe is observed. Large recirculation regions are formed in the rear region of the bubbles, thus creating a wake, which interacts with the following bubble. The flow containing a Taylor bubble and a liquid plug forms a structure that repeats itself intermittently throughout the flow, is known as the slug flow pattern [3].

In this work, it was studied the Taylor bubbles behavior for different gas and liquid superficial velocities. The analysis was performed by means the use of wire-mesh data and high-speed images. Hence, it was hypothesized the influence of the size, shape and population of the dispersed bubbles on both, the Taylor bubbles and liquid plug velocities.

Methodology

A scheme of the two-phase facility is shown in Fig. 1. The experimental setup consists mainly of an acrylic 0.026-m ID, 14-m long vertical pipe. The

water was circulated by using a pump (TH-40/160(R) powered by a frequency inverter for rotation control and measured by an electromagnetic flowmeter, while the air was supplied by an air compressor. The flows of both phases were monitored by Coriolis meters (Yokogawa). Two meters were used for the gas phase: one for low flow rates and another for high ones. At the entrance of the test section a 10m-long horizontal segment with the same internal diameter that the test section was assembled. The experiments were carried out for different flow conditions within the slug flow envelope. Both the air (J_G) and liquid (J_L) superficial velocities were increased from 0.2 m/s to 1.5 m/s and the mixing velocity was defined as $J = J_G + J_L$. Based on the J_G/J_L ratio, the experimental points were binned into three groups, as shown in Table 1. It has to be pointed out that these points correspond to the slug flow configuration.

Table 1. Experimental points classified by their J_G/J_L ratio

J_G/J_L =1	J_G/J_L <1	J_G/J_L >1
P01	P02	P03
P04	P05	P06
P07	P08	P09
P10	P11	P12
P13	P14	P15
P16	P17	P18

The gas flow characteristics were measured by a wire-mesh sensor placed at z/D = 301 in the circular test section. In the proximity of the wire-mesh sensor at z/D =281, a high-speed camera (MotionPro X3) was installed to visualize the flow. The images were captured at a 1040 fps over a recording period around 30s, with a resolution of 1280 x 1024 pixels.

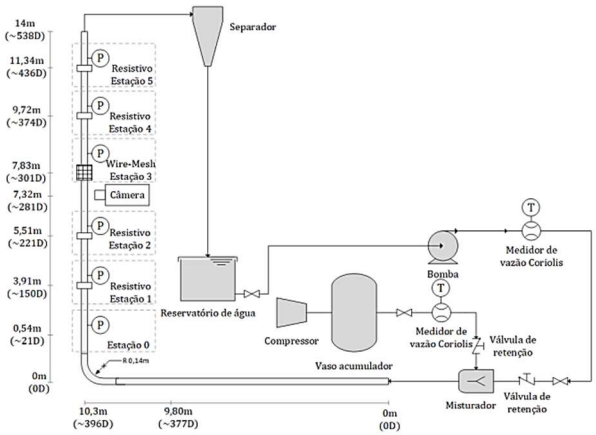

Figure 1. Experimental setup. The positions of the wire-mesh sensor and high-speed camera are shown.

This type of flow can be characterized by two dimensionless numbers. One of them is the Froude (Fr_J) number, which is given by:

$$\mathrm{Fr_J} = \frac{J}{\sqrt{gD}} \tag{1}$$

and the second one is the Reynolds number of the slug:

$$\mathrm{Re_J} = \frac{\rho_L J D}{\mu_L} \tag{2}$$

where g, D, ρ_L, μ_L, are gravity acceleration, pipe diameter, liquid density and liquid viscosity, respectively.

Results and Discussion

In Fig. 2, it is shown the behavior of the Taylor bubble nose as a function of the mixing velocity (J). It was observed that with the increase in the mixing velocity (J), that is, with higher Froude numbers, the round-shaped nose of the Taylor bubbles presented a pointed shape. This could be due to the increase in the velocity gradient, which becomes more visible and pronounced when velocities are higher, as it is the case of the points P15 and P17. Such behavior can be explained as a response to the large velocity fluctuations in the flow field but also by the influence of the wakes of the dispersed bubbles, which are strong enough to distort the bubbles' nose (Fig. 2). On the other hand, for low mixing velocities and consequently low Froude numbers, the bubble nose exhibits flatter shapes (i.e., P01, P02 and P08). Taylor bubbles with flatter noses are related to the low influence of the wake region of the preceding bubble's piston, which corresponds to small Reynolds numbers. This flattened shape is similar to the velocity profile expected in developed turbulent flow, without the influence of the agitation produced by the presence of dispersed bubbles.

It can be observed that by increasing the Froude number, the high mixture velocity induces instabilities leading to the breakup in the tails of the elongated bubbles and dispersed bubbles are therefore generated. However, it was also observed that as the ratio between the superficial velocity of the gas and the superficial velocity of the liquid increases (J>1) the population of small dispersed bubbles increase (Fig. 2). High concentrations of dispersed bubbles can be found along the Taylor bubbles (nose, body and rear) and in the liquid slug.

It is noted that as the Taylor bubbles rise due to the increase in the Reynolds and Froude numbers, the size and shape of the dispersed bubbles are modified.

In Fig. 3., it is observed that for dispersed bubbles at low Froude numbers, the inertial effects of the flow have minor influence and the bubbles present an ellipsoidal shape. As the Froude number increases, inertial effects become more pronounced, and spherical bubbles can be

observed (J≥1.2m/s). The latter effect can be related to the large shear stresses between the Taylor bubbles and the pipe wall. Additionally, the high shear stresses decrease the size of the dispersed bubbles.

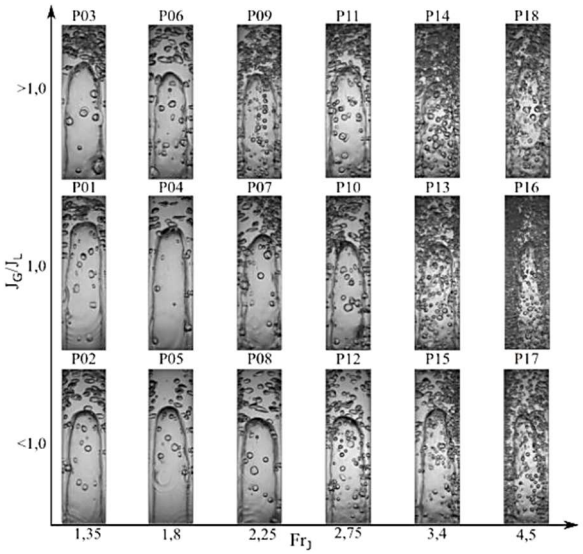

Figure 2. Taylor bubble noses for the different J_G/J_L ratios as a function of the Froude number.

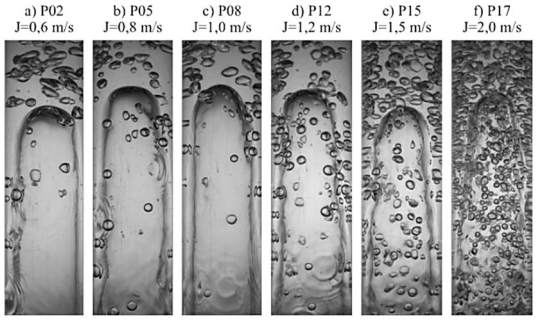

Figure 3. Detail of Taylor bubble noses for different J_G/J_L <1. The increase in dispersed bubble population can be noticed as well as the different shape patterns.

To analyze the sizes of the dispersed bubbles, only sample images located in the middle of the liquid piston were selected. This was done to avoid the influence of the wake region as well as the velocity profile in the proximity of the Taylor bubble nose. These images were disposed according to the Froude number and the J_G/J_L ratio, (Fig. 2).

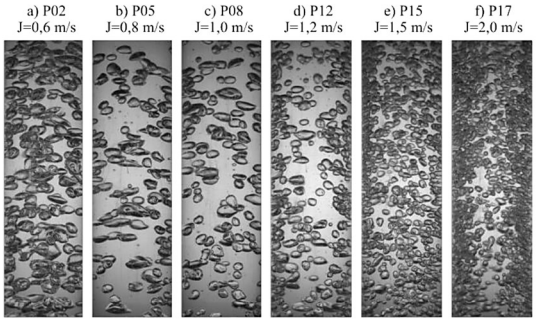

Figure 4. Dispersed bubbles in the slug region for different J_G/J_L <1.

The diameters were determined by processing images of a sample containing 20 dispersed bubbles for each experimental point. The equivalent diameters of the small bubbles were calculated, as follows:

$$d = (a^2 \cdot b)^{\frac{1}{3}} \quad (3)$$

where a is the major axis and b is the minor axis of an oblate spheroid. Figure 5 shows the values obtained as a function of the Reynolds number of the liquid piston.

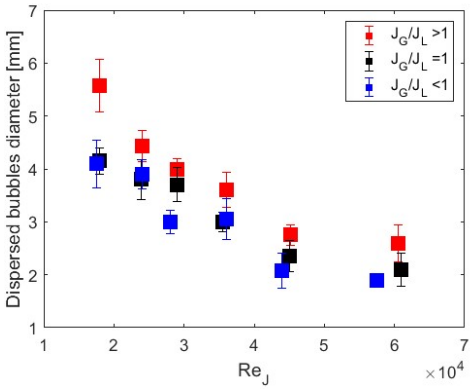

Figure 5. Dispersed bubble diameters for different J_G/J_L ratios as a function of the Reynolds number.

At expected, for higher piston Reynolds numbers, the diameters of the dispersed bubbles were smaller. This decrease in the diameter of the dispersed bubbles was observed for the three different J_G/J_L ratios. In addition, as the liquid velocity increased, that is, for points with $J_G/J_L \leq 1$, the dispersed bubbles were smaller for the same mixture velocity.

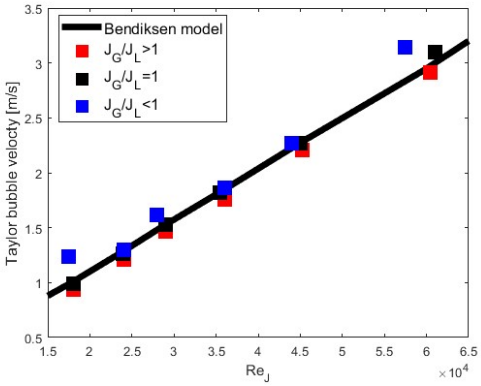

Figure 6. Mean Taylor bubble velocity for the different J_G/J_L ratios as a function of the Reynolds number, the Bendiksen model [4] was added as a comparison.

Figure 6 shows the response of the velocity of the Taylor bubbles as a function of the Reynolds number of the liquid slug. Clearly, the Taylor bubble velocities increase by increasing the mixing velocity. This can be attributed to the high flow inertia, for large Reynolds numbers. In addition, the Bendiksen model [4] was added as a comparison, the experimental data were used to obtain a linear regression and a correlation for the Taylor bubble velocity was obtained as:

$$\frac{V_{TB}}{\sqrt{gD}} = 1.25Fr_J + 0.1312 \quad (4)$$

It can be observed that the experimental results show good agreement with the correlation, but it is also important to point out that most of the points falling outside the trend correspond to the smaller diameters for the dispersed bubbles as shown in Fig. 5. From this, it can be hypothesized that the presence of such dispersed bubbles in the region between the elongated bubble and the liquid film near to the walls can generate a slip-lubrication effect and a low local density in the slug section, and both effects might contribute to the develop of larger Taylor bubble velocities.

Conclusions

The objective of this work was to experimentally characterize the slug flow in a vertical pipe. The experimental methodology herein described relied upon the use of an experimental circuit located at NUEM/UTFPR, with a 10-meter-long horizontal pipe, followed by a 14-m, 0.026-m vertical pipe where the experimental measurements were obtained. Air and water were used as working fluids and a wire-mesh sensor was used to obtain the Taylor bubbles' velocities. The test grid contained eighteen (18) flow combinations, grouped into six (6) different mixing speeds, binned as $J_G/J_L \leq 1 \geq J_G/J_L$.

From the images obtained with the high velocity camera, changes in the shape of the bubble front as a function of an increased Froude number were observed, whereas the increase in the Froude number was a consequence of an increased population of dispersed bubbles. The liquid agitation generated by the presence of such bubbles showed an influence on the shape of the Taylor bubble nose. Additionally, the size of the dispersed bubbles in the pistons was determined, showing the influence of the large shear stresses, which led to minor bubble sizes. From this latter outcome, it was supposed that the presence of the small bubbles would influence the Taylor bubble velocities, as demonstrated by an increase in the Reynolds numbers. Further analyses must be performed to validate such a hypothesis.

Acknowledgments

The authors would like to express their gratitude to NUEM-UTFPR and PRH21-ANP for their financial support.

Responsibility Notice

The authors are the only responsible for the content and opinions expressed in this article.

References

[1] Shoham, O. Mechanicstic modelling of gas-liquid two-phase flow in pipes. 1 Ed. SPE, 2006
[2] Taitel, Y. Barnea, D. Dukler, A. E. Modelling of flow pattern transitions for steady upward gas liquid flow in vertical tubes, AIChE Journal, vol. 26, pp 345-354,1980
[3] Taitel, Y., Barnea, D. Two-phase slug flow. Advances in Heat Transfer, vol. 20, pp 83-132,1990
[4] Bendiksen, K. H. An experimental investigation of the motion of long bubbles in inclined tubes. International Journal of Multiphase Flow, vol. 10, pp 476-483, 1984